

Robust quantum-like state simulation using *k*-regular bipartite networks

Xinjiang Zhou(周新疆), Tinggui Zhang(张廷桂)

Citation: Chin. Phys. B. 35, 090306 (2026). DOI: 10.1088/1674-1056/ae5c75 |
CSTR: 32038.14.CPB.ae5c75
http://cpb.iphy.ac.cn; http://iopscience.iop.org/cpb

What follows is a list of articles you may be interested in

Jensen-Shannon divergence coherence and its quantum speed limit

Jia-Rui Song(宋佳瑞), Chang-Shui Yu(于长水)
Chin. Phys. B. 35, 090301 (2026). DOI: 10.1088/1674-1056/ae1821 | CSTR: 32038.14.CPB.ae1821

Efficient semi-quantum private comparison protocol of size relation based on high-dimensional Bell states

Jie-Hui Huang(黄接辉), Mao-Long Li(李茂龙), Yan-Yan Liu(刘妍妍), Li-Guo Qin(秦立国), Li-Hua Gong(龚黎华)
Chin. Phys. B. 35, 080304 (2026). DOI: 10.1088/1674-1056/ae2abd | CSTR: 32038.14.CPB.ae2abd

Bipartite and tripartite entanglement in the two-qubit quantum Rabi model

Lijun Mao(毛丽君), Hongmei Wang(王红梅), Yaoyao Zhou(周瑶瑶), Hui Guo(郭慧)
Chin. Phys. B. 35, 080303 (2026). DOI: 10.1088/1674-1056/ae85f7 | CSTR: 32038.14.CPB.ae85f7

Hierarchy of average correlation, quantum steering and Bell nonlocality in two-qubit systems

Qinglong Tian(田清龙), Youneng Guo(郭有能)
Chin. Phys. B. 35, 080302 (2026). DOI: 10.1088/1674-1056/ae6b38 | CSTR: 32038.14.CPB.ae6b38

Nonadiabatic holonomic quantum computation in decoherence-free subspaces on Rydberg atoms

Ya Gao(郜雅), Meng-Le Guo(郭梦乐), Pei-Yao Song(宋佩瑶), Ji-Ze Han(韩济泽), Zhi-Guo Huang(黄智国), Jin-Lei Wu(吴金雷), Shi-Lei Su(苏石磊)
Chin. Phys. B. 35, 080301 (2026). DOI: 10.1088/1674-1056/ae6cce | CSTR: 32038.14.CPB.ae6cce

---

SPECIAL TOPIC — Quantum communication and quantum network

Robust quantum-like state simulation using k-regular bipartite networks

Xinjiang Zhou(周新疆) and Tinggui Zhang(张廷桂)†

School of Mathematics and Statistics, Hainan Normal University, Haikou 571158, *China*

(Received 8 January 2026; revised manuscript received 3 April 2026; accepted manuscript online 8 April 2026)

We establish a framework for constructing robust quantum-like states based on k-regular bipartite graphs, aiming to realize quantum-inspired information processing through classical oscillatory networks. We first introduce the k-regular bipartite graph and its mathematical representation, and analyze its intrinsic spectral properties. In contrast to ordinary k-regular non-bipartite graphs, the intrinsic bipartite symmetry, enhanced spectral gap, and global delocalization mechanism confer superior robustness to the emergent states. We verify that the emergent states of these bipartite graphs satisfy the axiomatic requirements of quantum-like states, and show that the global delocalization property ensures stable operation under structural noise. Based on the axiomatic requirements of quantum-like states, we further realize basic quantum-inspired gate operations in the classical network framework. Our numerical simulations reveal that the k-regular bipartite graph system exhibits enhanced coherence and stability under noise interference compared with non-bipartite graph systems. This research not only broadens the application boundaries of quantum-inspired computing but also provides a new feasible path for the practical implementation of classical simulation of quantum information processing.

Keywords: quantum-like states, k-regular bipartite networks, quantum coherence, quantum-inspired information processing

PACS: 03.67.Mn, 03.67.Hk

DOI: 10.1088/1674-1056/ae5c75 **CSTR:** 32038.14.CPB.ae5c75

1. Introduction

Quantum information theory represents one of the most promising frontiers in modern physics, offering novel paradigms for information processing that surpass the capabilities of classical computation.[1] By leveraging the unique features of quantum mechanics — such as superposition, entanglement, and quantum coherence — it enables groundbreaking advances in computing, communication, cryptography, and sensing.[2] Quantum resource theory (QRT) further formalizes and quantifies these advantages by identifying which quantum states and operations can be considered as "resourceful" and how they can be manipulated to perform tasks that are infeasible within classical frameworks.[3,4]

Despite its immense potential, the practical implementation of quantum technologies faces significant challenges.[5] Quantum states are inherently fragile and prone to decoherence due to interactions with the surrounding environment.[6,7] This sensitivity makes the preparation, preservation, and manipulation of high-fidelity quantum resources extremely difficult, especially in real-world conditions.[8] In contrast, classical systems are typically robust and easy to control; however, they lack the coherent dynamics that underpin the power of quantum information processing.

This fundamental distinction between quantum and classical systems has long defined the boundary between the two domains.[9,10] However, recent interdisciplinary studies across psychology,[11–14] biology,[15–17] chemistry,[18–20] and even social sciences[21–23] have revealed intriguing phenomena that resemble quantum behavior in classical settings. In particular, the pioneering work of Gregory D. Scholes and colleagues has demonstrated that complex classical networks can support stable and robust states that exhibit properties analogous to those of quantum systems.[24–27] These so-called quantum-like states not only mimic essential quantum characteristics but also display resilience against environmental perturbations, making them promising candidates for simulating quantum information processing in classical environments. Their research has opened a new avenue for exploring the intersection of classical complexity and quantum functionality.

Recent progress in quantum hardware and protocols further underscores the value of emulating quantum logic in controllable settings. For instance, generalized quantum measurement schemes have been developed in high-energy contexts,[28] while robust gate implementations — such as nonadiabatic holonomic quantum computation[29] and all-microwave CZ gates in fixed-frequency superconducting circuits[30] — highlight ongoing efforts to enhance coherence and operational fidelity. Although these approaches rely on genuine quantum platforms, they collectively emphasize a key insight: the *logical structure* of quantum information process-

†Corresponding author. E-mail: 2023120701000l4@hainnu.edu.cn

© 2026 Chinese Physical Society and IOP Publishing Ltd. All rights, including for text and data mining, AI training, and similar technologies, are reserved.

ing can be decoupled from its physical substrate. This motivates the exploration of purely classical systems that replicate such logical workflows while benefiting from inherent robustness.

Building on these insights, this work investigates a specific class of graph structures — k-regular bipartite graphs — as a platform for constructing robust quantum-like states. Our work makes two key contributions.

(1) **Theoretical construction** We rigorously prove that k-regular bipartite graphs satisfy all five axioms of quantum-like states, providing a new structure for constructing robust quantum-like states.

(2) **Numerical comparison and validation** Through controlled numerical simulations with parameters strictly aligned with previous work to ensure fairness, we verify that the bipartite structure exhibits significantly better coherence preservation and noise resilience than ordinary non-bipartite k-regular graphs.

We demonstrate that such graphs satisfy the axiomatic criteria proposed by Ref. [26] for quantum-like states, including distinguishability, stability under noise, and the presence of a well-defined spectral gap. Through rigorous spectral analysis, we show that these graphs maintain both structural integrity and functional stability even under various noisy conditions, thereby providing a solid foundation for simulating quantum dynamics in classical networks. Furthermore, our analysis of the resulting quantum-like coherence resources reveals a significantly higher degree of robustness compared to existing works based on non-bipartite graphs, a finding that is directly verified by our numerical simulation results.

In summary, this study bridges the conceptual gap between quantum and classical systems by establishing k-regular bipartite graphs as a robust platform for quantum-inspired information processing. Our results not only deepen the theoretical understanding of emergent quantum-like phenomena in classical networks but also offer a practical pathway toward developing noise-resilient alternatives for quantum information simulation tasks.

2. Preliminaries

2.1. Graphs and emergent states

Networks are mathematically represented by graphs, with their connectivity encoded in an adjacency matrix. In this work, we focus on k-regular bipartite graphs — a class of networks widely observed in resource allocation systems,[31] social networks,[32] and other complex systems.[33–35]

Definition 1 (k-regular bipartite graph[36]) Let $G = (U, V, E)$ be a bipartite graph with disjoint vertex sets U and V, and let E be the set of edges connecting vertices between U and V (i.e., no edges exist within U or within V). If every vertex $v \in U \cup V$ is connected by exactly k edges, then G is called a k-regular bipartite graph.

A fundamental property of k-regular bipartite graphs is that their adjacency spectrum is symmetric about the origin: if λ is an eigenvalue of the adjacency matrix, then $-\lambda$ is also an eigenvalue. This intrinsic bipartite symmetry lays the foundation for the robustness of the quantum-like states constructed based on such graphs.

The adjacency matrix $A \in \mathbb{R}^{n\times n}$ of graph G encodes its connectivity, where each entry $a_{ij} \in \{-1, 0, 1\}$ indicates the presence and type of edge between vertices i and j. The spectral properties of A, specifically its eigenvalues $\lambda_1, \ldots, \lambda_n$ and corresponding eigenvectors, determine the dynamical behavior of the system. To characterize the global spectral distribution of k-regular bipartite graphs, we adopt the density of states (DoS) formalism from condensed matter physics.

Definition 2 (density of states) The DoS of a graph's adjacency matrix A, denoted by $\rho(\lambda)$, is defined as

$$\rho(\lambda) = \frac{1}{n}\sum_{i=1}^{n} \delta(\lambda - \lambda_i), \tag{1}$$

where n is the total number of vertices in the graph; $\delta(\cdot)$ denotes the Dirac delta function, which forms a sharp peak at each eigenvalue λ_i; and λ is an arbitrary real number representing a possible eigenvalue.

Originating in quantum mechanics and condensed matter physics, where $\rho(\lambda)$ describes the distribution of energy levels, the DoS formalism is well-suited for characterizing the spectral distribution of graph adjacency matrices. In numerical practice, we approximate the Dirac delta function using a normalized histogram: we partition the eigenvalue spectrum into evenly spaced bins, count the number of eigenvalues falling into each bin, and normalize the counts such that the total area under the histogram equals 1, yielding an empirical estimate of $\rho(\lambda)$.

2.2. Quantum-like states

Recent advances in quantum-like systems have demonstrated that non-quantum physical platforms — including photonic lattices,[37] superconducting circuits,[38,39] neural networks,[40] and coupled oscillators[41] — can exhibit dynamics formally analogous to quantum phenomena such as superposition and entanglement. Although these systems do not rely on fundamental genuine quantum principles (e.g., wavefunction collapse), their mathematical structures enable the simulation of quantum-like behaviors, supporting quantum-inspired information processing tasks.

To ensure that quantum-like states can be constructed and that quantum-inspired operations can be implemented within classical systems, the following axiomatic requirements for quantum-like states and their underlying graph structures have been proposed in the pioneering work.[25]

(1) Emergent state in the spectral gap The graph structure should support an emergent state that is spectrally isolated from other states, forming a clear spectral gap.

(2) Robustness and stability under disorder The system should maintain its functional integrity under structural and parametric noise (e.g., edge removal, frequency fluctuations).

(3) Two distinguishable "on" states The core unit (quantum-like bit) should have two distinct, non-trivial states, neither of which corresponds to an inactive ("off") state. This is because quantum-like states rely on active network dynamics, and the quantum-like bit is defined through the interaction of oscillatory networks rather than a ground state (vacuum) and excited state.

(4) Definable unitary operations Basic unitary transformations should be implementable on the graph and its subgraphs, enabling the emulation of quantum-like logic operations.

(5) Coupling capability for superposition The system should allow coupling of multiple subgraphs such that the resulting state space supports superposition-like behaviors, analogous to quantum superposition.

This axiomatic framework provides a rigorous foundation for constructing quantum-like states in classical networks, ensuring that the resulting states satisfy the essential criteria for reliable quantum-inspired information processing.

3. Constructing quantum-like states

To ensure a fair comparison with existing studies on ordinary non-bipartite regular graphs, we strictly align our numerical parameters with established setups: we use a subgraph node count $n = 200$ to match the overall network scale, test the regular degree $k = 40$ to ensure structural consistency, employ a sample size of 10000 graphs to guarantee statistical reliability, and adopt consistent noise types. Edge addition and edge deletion have been considered in relevant literature; we further supplement edge-flipping noise to ensure comprehensive and consistent perturbation definitions.

In this section, we randomly construct a number of large k-regular bipartite graphs. Spectral analysis of these graphs reveals that certain special states (extremal eigenvalues) are clearly separated from the rest of the spectrum.

It is known from existing theoretical results[42] that random k-regular bipartite graphs are asymptotically Ramanujan graphs, so that non-trivial eigenvalues are bounded by $2\sqrt{k-1}$. This guarantees a large spectral gap between the extremal eigenvalues $\pm k$ and the bulk spectrum, which provides a theoretical basis for the robust emergent states observed in our numerical experiments. These states, referred to as emergent states, correspond to nontrivial dynamical or topological features on the graph. In fact, such states are characteristic of expander graphs, which exhibit strong global connectivity across the entire network and represent optimal structures for communication and walk-based processes.

Figure 1 presents the spectral analysis of several k-regular bipartite graphs with $n = 200$ vertices. The spectrum of an undirected graph can be interpreted as a coupling map of the eigenvalues associated with its adjacency matrix, reflecting the spectral relationships between connected vertices. Emergent states are clearly visible as isolated extremal eigenvalues — either maximum or minimum — in the spectrum. In our framework, an emergent quantum-like state corresponds to an eigenvalue that is spectrally isolated from the bulk of the spectrum. Specifically, the eigenvector associated with the largest eigenvalue ($\lambda = k$) is uniform over all vertices, taking the form $(1,1,\ldots,1)/\sqrt{n}$. Conversely, the eigenvector for the smallest eigenvalue ($\lambda = -k$) displays a clear bipartite signature: $(1,\ldots,1,-1,\ldots,-1)/\sqrt{n}$, where the sign pattern directly reflects the two disjoint vertex partitions of the graph.

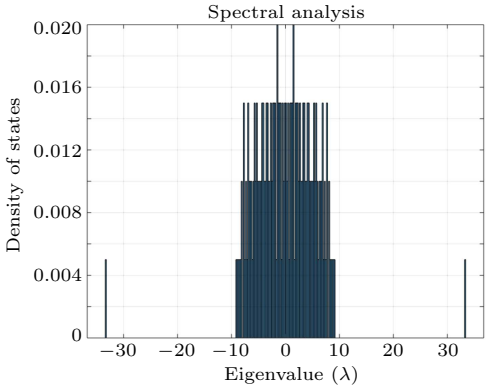


Fig. 1. Spectral analysis of several k-regular bipartite graphs with $n = 200$ and $k = 40$.

These emergent states, arising from global coherence rather than local details, provide a natural basis for encoding information in oscillator networks across domains such as neuroscience and social dynamics. As supported by existing theoretical results,[42,43] the spectral gap and global connectivity of k-regular bipartite graphs (asymptotically Ramanujan and expander graphs) inherently contribute to the stability of these emergent states, which is further verified by our numerical observations.

Figures 2–4 present the spectral analysis of k-regular bipartite graphs on $n = 200$ vertices under three types of structural noise: edge flipping, edge deletion, and edge addition. These disturbances mimic realistic imperfections including data loss, environmental fluctuations, and system fabrication errors. Despite such structural perturbations, the core spectral properties of the graphs remain largely intact, and the emergent states stay clearly separated from the bulk spectrum. This demonstrates strong robustness against random noise, which aligns with theoretical results from Refs. [42,43]: the inherent spectral gap and global delocalization of k-regular bipartite

graphs render their key spectral features insensitive to small structural variations, thus validating the reliability of our numerical observations.

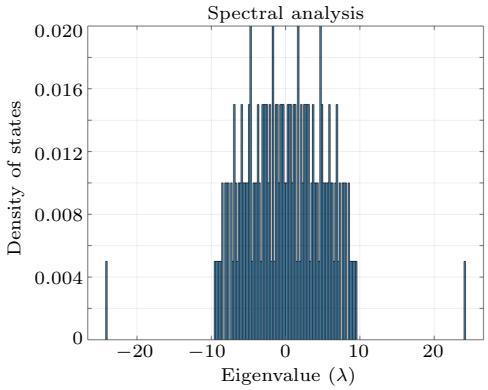


Fig. 2. Spectral analysis of k-regular bipartite graphs on $n = 200$ vertices under structural noise of edge flipping edge flipping with $P = 0.1$.

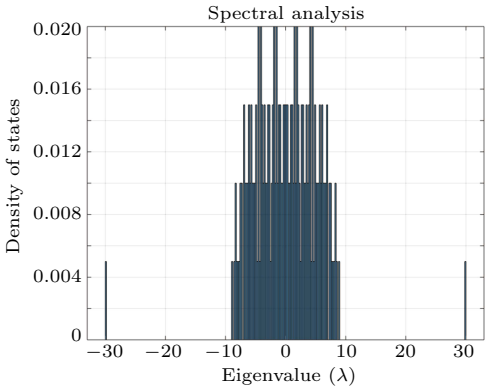


Fig. 3. Randomly add 400 edges.

The degree of separation of the emergent state is closely related to the spectral gap of the graph, defined as the difference between the largest and second-largest eigenvalues of the adjacency matrix. To evaluate the robustness of this property, we randomly generated 10000 k-regular bipartite graphs and measured their spectral gaps before and after applying various types of structural noise. As theoretically expected from the Ramanujan property of random k-regular bipartite graphs,[42] the original graphs exhibit a large average spectral gap, which provides a solid foundation for the spectral isolation of emergent states. The average spectral gaps were found to be 24.2168 (original graphs), 17.3729 (with edge flipping noise), 20.6561 (with edge deletion noise), and 27.7418 (with edge addition noise), with corresponding standard deviations of 0.2629, 0.4183, 0.2542, and 0.2691, respectively. Notably, even under structural perturbations, the spectral gaps remain sufficiently large to maintain the spectral isolation of emergent states, and the small standard deviations (all below 0.5) indicate high statistical consistency across the 10000 sample graphs. These results, presented in Fig. 5, demonstrate that the emergent states observed in Figs. 1–4 are statistically stable and not due to random fluctuations, further validating the reliability of our numerical simulations and the inherent robustness of k-regular bipartite graphs.

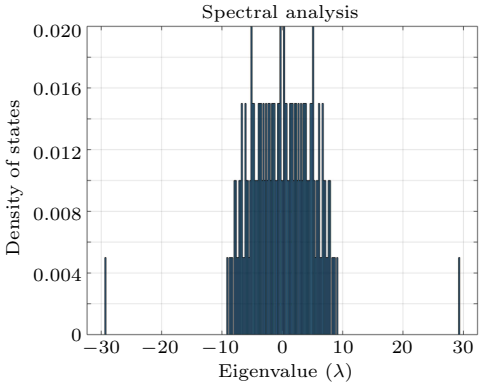


Fig. 4. Randomly remove 400 edges.

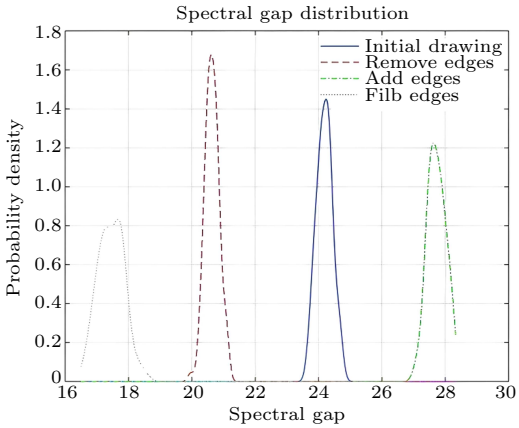


Fig. 5. Spectral gap distribution of 10000 random k-regular bipartite graphs before and after various structural noise perturbations.

The preceding analysis demonstrates that k-regular bipartite graphs exhibit emergent states in their spectra and remain robust and stable under structural disorder, thereby satisfying Axioms 1 and 2 of the quantum-like state requirements. This achievement directly builds on the theoretical advantages of k-regular bipartite graphs (Ramanujan and expander properties), where the inherent spectral gap and global connectivity ensure the stability of emergent states — advantages that are further confirmed by our statistical numerical results. Axiom 3 imposes certain constraints on our construction, particularly regarding the requirement for two distinguishable "on" states. Nevertheless, this framework remains broadly applicable across various fields such as network science, communication systems, chemistry, and biology. For instance, in the study by Ref. [39], k-regular bipartite graphs were employed to enhance information propagation mechanisms in graph neural networks. Leveraging the favorable properties of these classical network structures, we can observe emergent states arising from interactions among vertices (nodes), further supporting the potential of quantum-like state models in describing complex dynamical behaviors.

For a system composed of $2n$ oscillators arranged in a k-regular bipartite graph structure, the emergent states correspond to the maximum and minimum eigenvalues of the adjacency matrix, namely, k and $-k$, respectively. As known from

spectral graph theory, such extremal eigenvalues are well separated from the bulk spectrum in random k-regular bipartite graphs, providing a theoretical basis for the stability of these global modes. The corresponding eigenvectors are

$$\boldsymbol{p}_0 = \frac{1}{\sqrt{2n}}(1,1,\ldots,1), \quad \boldsymbol{p}_1 = \frac{1}{\sqrt{2n}}(1,\ldots,1,-1,\ldots,-1). \tag{2}$$

These two states represent coherent, global modes of oscillation across the entire network and serve as the basis states for the quantum-like bit. They are spectrally isolated from the remainder of the eigenvalue spectrum, thereby fulfilling Axiom 1's requirement for an emergent state, even under noisy conditions. To satisfy Axiom 4, we define a unitary transformation on the network. The effect of this unitary operation on the two emergent states $\boldsymbol{p}_0$ and $\boldsymbol{p}_1$ is given by[26]

$$U_{\rm cb}\boldsymbol{p}_0 = \begin{pmatrix}\mathbf{1}_n\\ \mathbf{0}_n\end{pmatrix}, \quad U_{\rm cb}\boldsymbol{p}_1 = \begin{pmatrix}\mathbf{0}_n\\ \mathbf{1}_n\end{pmatrix}. \tag{3}$$

The matrix $U_{\rm cb}$ is represented as

$$U_{\rm cb} = \frac{1}{\sqrt{2n}}\begin{bmatrix}\mathbf{1}_n & \mathbf{1}_n\\ \mathbf{1}_n & -\mathbf{1}_n\end{bmatrix}. \tag{4}$$

This transformation maps the global coherent modes of the network into distinguishable computational basis states, thereby enabling the interpretation of graph-based states as quantum-like bits. In this framework, the state of the entire system resembles the $|+\rangle$ state. When the connecting edge takes the value -1, the state becomes analogous to the $|-\rangle$ state. Due to the inherent symmetry of the system, these states cannot be intuitively distinguished without additional processing. Therefore, a unitary operation is required to reveal and manipulate this distinction effectively. This construction leverages the bipartite structure and its spectral properties to emulate quantum state distinguishability in a classical network setting.

Given the mapping from emergent states to the standard computational basis via the unitary transformation $U_{\rm cb}$, as defined in Eq. (3), we can now define quantum-like gate operations on graph states. Specifically, for a generic quantum gate U_g acting on qubits, its counterpart operation on the graph state can be expressed as

$$U_g = U_{\rm cb}^{-1}(V_g \otimes \mathbf{1}_{2n})U_{\rm cb}. \tag{5}$$

We now illustrate how standard single-qubit quantum gates can be realized as operations on the emergent states of a k-regular bipartite graph. For each gate, we specify its action in the computational basis via a 2×2 matrix V_g, and then lift it to the full graph space using the conjugation formula in Eq. (5).

The Pauli-X gate, defined by

$$V_X = \begin{pmatrix}0 & 1\\ 1 & 0\end{pmatrix}, \tag{6}$$

implements a bit-flip between the quantum-like bit basis states. Its action on the emergent eigenvectors is given by

$$U_g^{(X)}\boldsymbol{p}_0 = \begin{pmatrix}\mathbf{0}_n\\ \mathbf{1}_n\end{pmatrix}, \quad U_g^{(X)}\boldsymbol{p}_1 = \begin{pmatrix}\mathbf{1}_n\\ \mathbf{0}_n\end{pmatrix}. \tag{7}$$

This operation swaps the dominant oscillatory activity between the two partitions of the bipartite graph, mirroring the role of the X-gate in quantum computing. The corresponding operator on the full $2n$-dimensional space is

$$U_g^{(X)} = \frac{1}{2n}\begin{bmatrix}\mathbf{0}_{2n} & \mathbf{1}_{2n}\\ \mathbf{1}_{2n} & \mathbf{0}_{2n}\end{bmatrix}. \tag{8}$$

The Pauli-Y gate introduces both a bit-flip and a relative phase shift, with

$$V_Y = \begin{pmatrix}0 & -\mathrm{i}\\ \mathrm{i} & 0\end{pmatrix}. \tag{9}$$

Its lifted action reads

$$U_g^{(Y)}\boldsymbol{p}_0 = \begin{pmatrix}\mathbf{0}_n\\ \mathrm{i}\,\mathbf{1}_n\end{pmatrix}, \quad U_g^{(Y)}\boldsymbol{p}_1 = \begin{pmatrix}-\mathrm{i}\,\mathbf{1}_n\\ \mathbf{0}_n\end{pmatrix}, \tag{10}$$

which simultaneously exchanges the partitions and imparts a $\pi/2$ phase difference between them. Such phase-sensitive operations are enabled by the well-defined spectral structure of k-regular bipartite graphs, ensuring stable and predictable dynamics. The full-space representation is

$$U_g^{(Y)} = \frac{1}{2n}\begin{bmatrix}\mathbf{0}_{2n} & -\mathrm{i}\,\mathbf{1}_{2n}\\ \mathrm{i}\,\mathbf{1}_{2n} & \mathbf{0}_{2n}\end{bmatrix}. \tag{11}$$

The Pauli-Z gate applies a phase flip to the $|1\rangle$ state:

$$V_Z = \begin{pmatrix}1 & 0\\ 0 & -1\end{pmatrix}. \tag{12}$$

On the graph, it acts as

$$U_g^{(Z)}\boldsymbol{p}_0 = \begin{pmatrix}\mathbf{1}_n\\ \mathbf{0}_n\end{pmatrix}, \quad U_g^{(Z)}\boldsymbol{p}_1 = \begin{pmatrix}\mathbf{0}_n\\ -\mathbf{1}_n\end{pmatrix}, \tag{13}$$

leaving the amplitude distribution unchanged but reversing the sign of oscillations in the second partition — thus implementing a symmetry-preserving phase rotation. This symmetry-preserving property is inherently supported by the bipartite structure of the graph, ensuring that the phase operation does not disrupt the spectral isolation of emergent states. Its matrix form is

$$U_g^{(Z)} = \frac{1}{2n}\begin{bmatrix}\mathbf{1}_{2n} & \mathbf{0}_{2n}\\ \mathbf{0}_{2n} & -\mathbf{1}_{2n}\end{bmatrix}. \tag{14}$$

Finally, the Hadamard gate generates an equal superposition of the computational basis states:

$$V_H = \frac{1}{\sqrt{2}}\begin{pmatrix}1 & 1\\ 1 & -1\end{pmatrix}. \tag{15}$$

Its action on the emergent modes yields

$$U_g^{(H)}\boldsymbol{p}_0 = \frac{1}{\sqrt{2}}\begin{pmatrix}\mathbf{1}_n\\ \mathbf{1}_n\end{pmatrix}, \quad U_g^{(H)}\boldsymbol{p}_1 = \frac{1}{\sqrt{2}}\begin{pmatrix}\mathbf{1}_n\\ -\mathbf{1}_n\end{pmatrix}, \tag{16}$$

coherently redistributing oscillatory energy across both partitions and enabling the creation of superposed quantum-like states analogous to $|+\rangle$ and $|-\rangle$. This coherent redistribution is feasible due to the global connectivity and spectral gap of k-regular bipartite graphs, which support stable superposition states even in the presence of minor structural perturbations. The associated operator is

$$U_g^{(H)} = \frac{1}{2n}\begin{bmatrix}\mathbf{1}_{2n} & \mathbf{1}_{2n}\\ \mathbf{1}_{2n} & -\mathbf{1}_{2n}\end{bmatrix}. \tag{17}$$

These constructions demonstrate that fundamental quantum logic operations can be faithfully implemented on classical k-regular bipartite graphs through spectral engineering, thereby establishing a concrete bridge between network dynamics and quantum information primitives. Consistent with the theoretical properties of expander graphs, the global connectivity of k-regular bipartite graphs ensures that these quantum-like operations are robust and reproducible, further validating the practicality of our graph-based framework.

When multiple k-regular bipartite graphs are coupled together, the resulting composite system resides in a tensor product space formed by the individual Hilbert spaces of each graph. Consider N such graphs $\{G^{(q)}\}_{q=1}^{N}$, each of size n, with corresponding adjacency matrices $A^{(q)}$. The two dominant eigenvectors of each subgraph $G^{(q)}$, associated with the largest and smallest eigenvalues $\pm k$, are denoted as $|0_q\rangle$ and $|1_q\rangle$, respectively. The total system can be represented as the Cartesian product (denoted by $\square$) of these subgraphs:[44]

$$G = \bigsquare_{q=1}^{N} G^{(q)}, \tag{18}$$

where $\square$ denotes the Cartesian graph product. This Cartesian product construction preserves the key spectral properties of individual k-regular bipartite graphs, ensuring that the composite system maintains the same robustness and quantum-like characteristics as its constituent subgraphs. This formulation enables the construction of complex composite systems from simpler building blocks, providing a structured framework for studying emergent behavior and applying quantum-like operations on graph-based states.

The joint adjacency matrix of the entire system is defined as the sum of tensor products of individual adjacency matrices:

$$R_{N_{\mathrm{QL}}} = \sum_{q=1}^{N_{\mathrm{QL}}}\left(\mathbf{1}_{2n}^{\otimes(q-1)}\otimes R^{(q)}\otimes\mathbf{1}_{2n}^{\otimes(N_{\mathrm{QL}}-q)}\right), \tag{19}$$

where $R^{(q)}$ is given by

$$R^{(q)} = \begin{pmatrix}A^{(q)} & C^{(q)}\\ C^{(q)} & A^{(q)}\end{pmatrix}. \tag{20}$$

Here, $C^{(q)}$ represents a symmetric non-simple graph (allowing self-loops) with valency l. This coupling structure introduces inter-graph interactions while preserving the internal symmetry of each subgraph.

The emergent states of the overall system are formed as tensor products of the individual quantum-like bit states. Then a generic computational basis state of the composite system can be written as

$$|s_1 s_2 \cdots s_N\rangle = |s_1\rangle\otimes|s_2\rangle\otimes\cdots\otimes|s_N\rangle, \tag{21}$$

where $s_q \in \{0,1\}$. This tensor product structure ensures that the composite system maintains a well-defined Hilbert space structure, where the state space of the entire system is homomorphic to the tensor product of individual subgraph state spaces. This directly fulfills the requirement of Axiom 5, which defines the conditions for constructing superposition-compatible state spaces.

By appropriately defining the coupling mechanisms between subgraphs, we can construct arbitrary superpositions of such product states. Leveraging the favorable spectral properties of k-regular bipartite graphs as expander graphs, this composite framework ensures that superposition states remain stable under structural perturbations, further validating the feasibility of our construction.

For instance, consider a system composed of $N_{\mathrm{QL}} = 2$ subgraphs. The resulting adjacency matrix takes the form

$$R_{N_{\mathrm{QL}}} = R^{(1)}\otimes\mathbf{1}_{2n} + \mathbf{1}_{2n}\otimes R^{(2)}, \tag{22}$$

which reflects the independent contributions of each subgraph to the overall structure. To generate different two-particle quantum-like states, we can manipulate the matrix $C^{(q)}$, which introduces additional intra-subgraph connections or self-loops. By varying $C^{(q)}$, we can explore a range of composite system behaviors and emergent phenomena, demonstrating the flexibility and expressiveness of this graph-based framework.

Figure 6 illustrates the scenario in which there are no additional connections ($C^{(q)} = 0$) between subsystems. In this case, the system reduces to

$$R^{(q)} = \begin{pmatrix}A^{(q)} & 0\\ 0 & A^{(q)}\end{pmatrix}. \tag{23}$$

Specifically, $A^{(1)}$ is the adjacency matrix of a k-regular bipartite graph with $k = 40$ and partition size $n = 200$, while $A^{(2)}$ corresponds to a k-regular bipartite graph with $k = 20$ and the same partition size $n = 200$. This configuration represents a decoupled system, where each subsystem evolves independently according to its own adjacency matrix. The emergent states, ordered from right to left, are $|0_1 0_2\rangle$, $|0_1 1_2\rangle$, $|1_1 0_2\rangle$, and $|1_1 1_2\rangle$. The spectral distribution in Fig. 6 confirms that these tensor product states are spectrally isolated, verifying that the system can support coherent superposition states as required by Axiom 5.

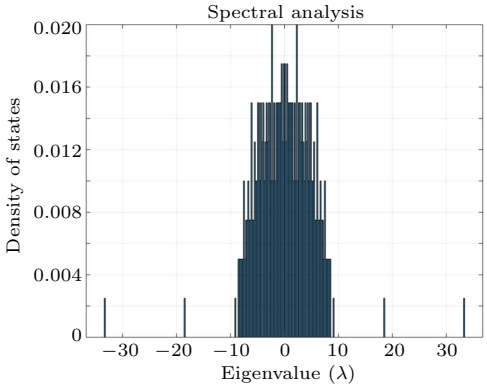


Fig. 6. Spectral analysis of the decoupled composite system ($C^{(q)} = 0$), showing clear spectral isolation of the four emergent states corresponding to the tensor product basis $|0_1 0_2\rangle, |0_1 1_2\rangle, |1_1 0_2\rangle, |1_1 1_2\rangle$.

In analogy with quantum mechanics, we define four maximally entangled quantum-like states using graph couplings:

$$\begin{aligned} |\Phi^+\rangle &= \frac{1}{\sqrt{2}}\left(|0_1 0_2\rangle + |1_1 1_2\rangle\right), \\ |\Phi^-\rangle &= \frac{1}{\sqrt{2}}\left(|0_1 0_2\rangle - |1_1 1_2\rangle\right), \\ |\Psi^+\rangle &= \frac{1}{\sqrt{2}}\left(|0_1 1_2\rangle + |1_1 0_2\rangle\right), \\ |\Psi^-\rangle &= \frac{1}{\sqrt{2}}\left(|0_1 1_2\rangle - |1_1 0_2\rangle\right). \end{aligned} \tag{24}$$

These states can be realized by appropriately choosing $C^{(q)}$ to introduce controlled interactions between the subsystems. For example, Fig. 7 shows a Bell-like state $|\Phi^+\rangle$ generated by a specific design of $C^{(q)}$. The emergent states, labeled from right to left in the spectrum, correspond to $|0_1 0_2\rangle$ and $|1_1 1_2\rangle$, respectively. The clear spectral separation observed in the spectrum confirms that the coupled graph structure supports stable entangled superpositions, as required for quantum-like information processing.[25,26] This capability not only demonstrates the expressive power of the model but also verifies Axiom 5, which requires that coupled graphs form a space compatible with superpositions of product states.

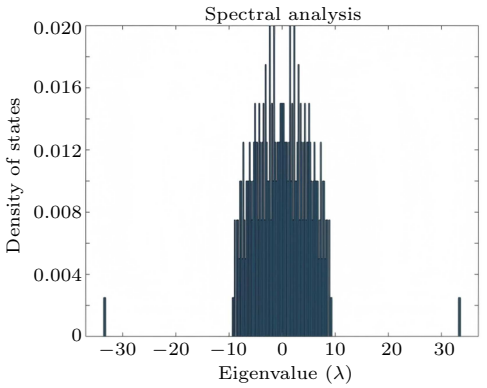


Fig. 7. Spectral analysis of the coupled composite system with $C^{(q)} \neq 0$, demonstrating the realization of a Bell-like entangled quantum-like state.

Furthermore, the unitary operations previously defined — such as those corresponding to single-quantum-like bit gates — can be naturally extended to act on these superposition states. This enables the definition of multi-quantum-like bit operations within the graph-based framework. This extensibility follows the standard paradigm of quantum-like state construction established in previous work,[24,27] ensuring consistency with the axiomatic requirements. As an illustrative example, consider the controlled-NOT (CNOT) gate, which operates on two quantum-like bits: one serving as the control and the other as the target. In standard quantum computing, the CNOT gate is defined as

$$\mathrm{CNOT}\,|c\rangle|t\rangle = |c\rangle|t \oplus c\rangle, \tag{25}$$

where $\oplus$ denotes addition modulo 2.

In our framework, this operation can be implemented by constructing a suitable unitary operator that acts on the tensor product space of two subgraphs. Specifically, the CNOT-like operation on quantum-like bits is expressed as

$$U_{\mathrm{CNOT}} = U_{\mathrm{cb}}^{-1}\left(V_{\mathrm{CNOT}} \otimes \mathbf{1}_{2n}^{\otimes(N-2)}\right) U_{\mathrm{cb}}, \tag{26}$$

where V_{CNOT} denotes the standard matrix representation of the CNOT gate:

$$V_{\mathrm{CNOT}} = \begin{pmatrix} 1 & 0 & 0 & 0 \\ 0 & 1 & 0 & 0 \\ 0 & 0 & 0 & 1 \\ 0 & 0 & 1 & 0 \end{pmatrix}. \tag{27}$$

This construction ensures that quantum-like operations preserve the structure of the underlying Hilbert space and enable the generation of entangled states across different quantum-like bits — mirroring the behavior of entangling gates in standard quantum computing. By extending unitary operations to composite graph systems, we realize a complete set of quantum-like logic primitives, consistent with the principles of quantum-inspired information processing.[42]

Through the preceding analysis, we have demonstrated that certain classical networks based on k-regular bipartite graphs satisfy all five axioms required for constructing quantum-like states. This finding leads to the following theorem.

Theorem 1 k-regular bipartite graphs satisfy all five axioms of quantum-like states, thus enabling the construction of robust quantum-like states in classical network systems.

4. Quantum-like coherent resources

According to the theory of quantum resource theory,[2] the essential components for quantum operations are free states, free operations, and resources. Free states refer to those that can be freely accessed at any time, while free operations — those that map free states to free states — are generally considered easy to implement. The key component is the resource, which includes, but is not limited to, quantum entanglement and quantum coherence. These resources are crucial

for enabling applications such as quantum-inspired computing and quantum-inspired information processing. As an example, quantum coherence refers to the ability of a quantum system to maintain well-defined phase relationships in its wavefunction, reflecting the wave-like nature of quantum states. However, this type of quantum resource is fragile — it is easily degraded by environmental noise and fluctuations, a process known as decoherence. As documented in experimental and theoretical studies,[6–8] decoherence remains a major obstacle to stable quantum information processing in genuine quantum systems. In contrast, the coherence resource obtained from quantum-like states constructed using k-regular bipartite graphs exhibits robustness against such disturbances. This robustness enables more reliable utilization of coherence in quantum-inspired information processing tasks.

The density matrix ρ is constructed from the set of eigenvectors of the adjacency matrix of a k-regular bipartite graph. The quantum-like resources obtained from such graph-based systems can be evaluated from two perspectives. First, the states we consider are globally coherent and exhibit a phenomenon known as coherent delocalization. This delocalization property is one of the core intrinsic mechanisms that endow the bipartite structure with enhanced robustness, as we will demonstrate in the following analysis. A commonly used measure for quantifying localization or delocalization is the inverse participation ratio (IPR): smaller IPR values indicate stronger delocalization, while larger values correspond to more localized states. The IPR of a density matrix ρ is defined as

$$\mathrm{IPR}(\rho) = \sum_i \rho_{ii}^2, \tag{28}$$

where ρ_{ii} denotes the diagonal elements of ρ. The IPR measure has been widely adopted in complex networks and quantum dynamics to characterize state localization properties.

Second, the strength of coherence itself serves as a crucial resource. To quantify this, we consider the distance between ρ and its nearest incoherent state, which is obtained by setting all off-diagonal entries of ρ to zero and denoted as $\sigma = \mathrm{diag}(\rho)$. This distance can be characterized using quantum relative entropy, which provides a precise evaluation of how much ρ deviates from an incoherent state, thereby quantifying the amount of coherence present. The quantum relative entropy between two density matrices ρ and σ is defined as

$$S(\rho \,\|\, \sigma) = \mathrm{Tr}(\rho \log_2 \rho) - \mathrm{Tr}(\rho \log_2 \sigma), \tag{29}$$

where ρ represents the full quantum-like state and σ corresponds to the incoherent reference state derived from ρ. This coherence metric is rooted in quantum resource theory and has been validated in both quantum and quantum-like systems.[2,45]

In this study, we examine the impact of noise in the form of edge deletion on quantum-like systems via numerical simulations. The density operator is altered as a result of edge removal, reflecting changes in the system's coherence properties. Let m denote the number of edges removed during the noise process. We define the relationship between c, m, n (number of nodes), and k (degree of regularity) as

$$c = \frac{2m}{nk}. \tag{30}$$

Figure 8 illustrates the IPR as a function of noise intensity c for both k-regular bipartite and non-bipartite graphs. It can be observed that when c is relatively low (approximately from 0 to 0.7), the IPR value remains close to zero, indicating that the wavefunction is uniformly distributed across the entire space and the system exhibits a highly delocalized state. As c approaches 0.8, the IPR begins to increase significantly, and when c nears 0.9, the IPR rises rapidly toward 1. This indicates that the wavefunction becomes increasingly localized within a smaller spatial region. Thus, at lower noise intensities ($c < 0.7$), the system remains in a delocalized state, while at $c \approx 0.8$, the system undergoes a critical transition where environmental noise starts to have a significant impact. At $c \approx 0.9$, the high noise intensity disrupts the extended nature of the wavefunction, leading to strong localization. In comparison, non-bipartite graphs show an earlier onset of localization and a more rapid increase in IPR, indicating weaker resistance to structural noise.

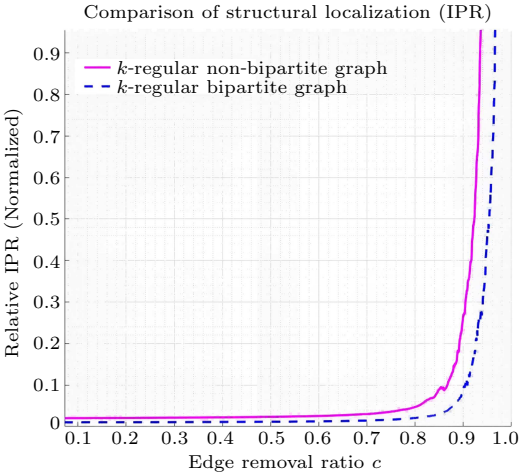


Fig. 8. IPR under edge-deletion noise, comparing k-regular bipartite and non-bipartite graphs from numerical simulations.

Figure 9 displays the relative entropy of coherence (KL divergence) for both bipartite and non-bipartite graphs with respect to the noise intensity c. When c is below approximately 0.6, the KL divergence remains at a high and relatively stable level, suggesting that the quantum-like coherence of the system is well preserved. As c approaches 0.7, the KL divergence begins to decrease significantly, marking the onset of decoherence. Around $c = 0.8$, the KL divergence drops sharply,

approaching zero, indicating that the superposition and coherence properties are severely degraded by the noise, and the system tends toward a classical or mixed state. Bipartite graphs clearly maintain higher coherence and delay the decoherence threshold more effectively than non-bipartite graphs under the same noise conditions.

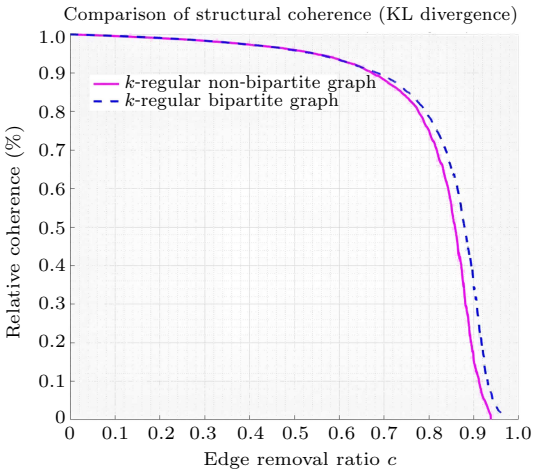


Fig. 9. Relative entropy of coherence under edge-deletion noise, comparing k-regular bipartite and non-bipartite graphs from numerical simulations.

Ordinary k-regular non-bipartite graphs were shown to maintain good purity and coherence in their quantum-like resources even when up to half of the edges were removed.[24] Notably, all numerical parameters in our study, including total network size, regularity degree $k = 40$, and noise types (edge addition and edge deletion), are strictly aligned with the benchmark setup to ensure a fair cross-structure comparison, where edge flipping is further supplemented in this work for a more comprehensive robustness evaluation.

In contrast, our k-regular bipartite networks exhibit significantly improved stability: the quantum-like coherence remains well-preserved even under a noise intensity of $c = 0.6$, substantially higher than the critical threshold observed in ordinary non-bipartite graphs. This enhanced robustness directly highlights the unique advantage of bipartite structures in constructing resilient quantum-inspired resources.

5. Conclusion and outlook

We have demonstrated that k-regular bipartite graphs can support spectrally isolated emergent states that fully satisfy the axiomatic requirements for quantum-like states. Quantum-like states remain stable under structural noise, offering a reliable pathway to quantum-inspired information processing in classical networks.

Furthermore, the proposed framework exhibits high practical feasibility. First, large-scale k-regular bipartite graphs can be precisely implemented across various classical physical platforms. In this model, each vertex corresponds to a physical oscillator, which may be realized as an electronic oscillator in integrated circuits, a photonic mode in waveguides, or a mechanical oscillator in optomechanical systems. The edges of the graph correspond to the controllable coupling between these oscillators. Existing coupled oscillator hardware platforms, such as CMOS integrated oscillator arrays used for Ising machines, have already demonstrated programmable networks with over 1000 nodes and arbitrary topologies. Consequently, the uniform connection degree required by k-regular graphs can be easily satisfied by configuring identical coupling strengths for each node, enabling the practical construction of large-scale k-regular bipartite structures without the need for exotic fabrication techniques. Second, the unitary operations defined on graph states are physically realizable. These unitary transformations correspond to phase flipping of subgraph partitions and the controllable modulation of inter-subgraph coupling strength, capabilities that have been proven feasible in recent studies on classical oscillator-based quantum-like simulation. For example, single-qubit unitary gates, such as the Hadamard gate, can be implemented by precisely adjusting the relative phase and coupling strength between the two partitions of the bipartite graph. This process coherently redistributes oscillatory energy between the two global emergent modes (p_0 and p_1 in our framework) to generate the required superposition states. These operations are essentially linear mode transformations of the coupled system, which can be precisely controlled through electrical or optical modulation. Notably, all such manipulations can be performed at room temperature, avoiding the cryogenic conditions and fragile quantum resources demanded by genuine quantum systems, thereby significantly lowering the barrier for experimental implementation.

However, the absence of intrinsic quantum uncertainty means that security must be grounded in computational or topological complexity rather than physical quantum properties.

Future work will focus on: (i) optimizing graph structures to further enhance coherence preservation under high-noise environments; (ii) developing more efficient numerical simulation platforms to realize large-scale quantum-inspired information processing; and (iii) extending the framework to multi-component systems, enabling more complex information processing tasks that combine the robustness of classical networks with the logical expressiveness of quantum-like operations.

Acknowledgements

This work is supported by the specific research fund of the Innovation Platform for Academicians of Hainan Province and the Hainan Provincial Graduate Innovation Research Program (Grant No. Qhys2024-399).

References

[1] Galindo A and Martin-Delgado M A 2002 *Rev. Mod. Phys.* **74** 347
[2] Vasani V 2024 *J. Ind. Inf. Integr.* **37** 100594
[3] Chitambar E and Gour G 2019 *Rev. Mod. Phys.* **91** 025001
[4] Lami L 2018 *Phys. Rev. A* **98** 022335
[5] Schleich W P, Ranade K S, Anton C, Arndt M, Aspelmeyer M, Bayer M and Zoller P 2016 *Appl. Phys. B* **122** 1
[6] Schlosshauer M 2019 *Phys. Rep.* **831** 1
[7] Zurek W H 2003 *Rev. Mod. Phys.* **75** 715
[8] Memon Q A, Al Ahmad M and Pecht M 2024 *Quantum Rep.* **6** 627
[9] Blanchard Ph and Jadczyk A 1993 *Phys. Lett. A* **175** 157
[10] Paty M 2000 *Synthese* **125** 179
[11] Busemeyer J R and Wang Z 2015 *Curr. Dir. Psychol. Sci.* **24** 163
[12] Kyriazos T and Poga M 2024 *Biosystems* **235** 105070
[13] Adamski A 2011 *NeuroQuantology* **9** 563
[14] Bruza P D, Wang Z and Busemeyer J R 2015 *Trends Cogn. Sci.* **19** 383
[15] Khrennikov A, Iryama S, Basieva I, *et al.* 2024 *Biosystems* **242** 105261
[16] Lambert N, Chen Y N, Cheng Y C, Li C M, Chen G Y and Nori F 2013 *Nat. Phys.* **9** 10
[17] Kim Y, Bertagna F, D'Souza E M, Heyes D J, Johannissen L O, Nery E T and McFadden J 2021 *Quantum Rep.* **3** 80
[18] Cao Y, Romero J, Olson J P, Degroote M, Johnson P D, Kieferová M and Aspuru-Guzik A 2019 *Chem. Rev.* **119** 10856
[19] Shao Y, Molnar L F, Jung Y, Kussmann J, Ochsenfeld C, Brown S T and Head-Gordon M 2006 *Phys. Chem. Chem. Phys.* **8** 3172
[20] Bauer B, Bravyi S, Motta M and Chan G K L 2020 *Chem. Rev.* **120** 12685
[21] Trnka R 2018 *Millennium* **47** 87
[22] O'Brien K L 2016 *WIREs Clim. Change* **7** 618
[23] Van Langenhove L 2021 *Found. Sci.* **26** 55
[24] Scholes G D 2023 *Entropy* **25** 1519
[25] Scholes G D 2024 *Proc. R. Soc. A* **480** 20240209
[26] Scholes G D and Amati G 2025 *Phys. Rev. Lett.* **134** 060202
[27] Amati G and Scholes G D 2024 arXiv:2408.06485 [quant-ph]
[28] Wu S, Li H, Chen J and Zhang Y 2024 *Chin. Phys. Lett.* **41** 110301
[29] Su S L, Guo Q, Wang H F, Zhu A D and Zhang S 2024 *Chin. Phys. Lett.* **41** 040302
[30] Gao W, Liu Y, Li Z, Wang C X and Song F 2025 *Chin. Phys. B* **34** 040304
[31] Vishnevsky V M, Larionov A A and Ivanov R E *Proceedings of the 2016 Advances in Wireless and Optical Communications* 2016 IEEE pp. 221–224
[32] Malliaros F D, Megalooikonomou V and Faloutsos C 2015 *Knowl. Inf. Syst.* **45** 645
[33] Maragathavalli K, Jothi R M J and Thamizisai D 2026 *Sixth International Conference on Advances in Electrical, Computing, Communications and Sustainable Technologies (ICAECT)* 2026 IEEE pp. 1–6
[34] Demange M and Ekim T 2008 *Lect. Notes Comput. Sci.* **4978** 364
[35] Kunegis J 2015 *Internet Math.* **11** 201
[36] Bača M, Baskoro E T, Salman A N M, *et al.* 2011 *Bull. Math. Soc. Sci. Math. Roumanie* **54** 15
[37] Peruzzo A, Lobino M, Matthews J C F, Matsuda N, Politi A, Poulios K, Zhou X Q, Lahini Y, Ismail N, Wörhoff K, *et al.* 2010 *Science* **329** 1500
[38] Wang C, Zhang Y Y and Chen Q H 2012 *Phys. Rev. A* **85** 052112
[39] Zhang H, Sun Y and Zhang X 2026 *Adv. Quantum Technol.* **9** e00752
[40] Liu J, Lim K H, Wood K L, Huang W, Guo C and Huang H L 2021 *Sci. China Phys. Mech. Astron.* **64** 290311
[41] Babbush R, Berry D W, Kothari R, Somma R D and Wiebe N 2023 *Phys. Rev. X* **13** 041041
[42] Marcus A, Spielman D A and Srivastava N 2015 *Ann. Math.* **182** 307
[43] Alon N 1986 *Combinatorica* **6** 83
[44] Feder T 1992 *J. Graph Theory* **16** 467
[45] Baumgratz T, Cramer M and Plenio M 2014 *Phys. Rev. Lett.* **113** 140401